RADIATION EFFECTS ON THE MICROSTRUCTURAL STABILITY OF INTERACTION LAYER IN RERTR FUELS

B. D. Miller[1], J. Gan[2], T. R. Allen[1], D. D. Keiser[2], and D. M. Wachs[2]

[1] University of Wisconsin-Madison, Wisconsin, USA
[2] Idaho National Laboratory, Idaho Falls, Idaho, USA

Abstract

To provide information to address the concern of fuel-matrix interaction (FMI) in current RERTR fuels, three depleted uranium alloys were cast to simulate the phases seen in the FMI formed interaction zones. SEM analysis indicates the following phases: $U(Al,Si)_3$, $(U,Mo)(Al,Si)_3$, UMo_2Al_{20}, UAl_4, and $U_6Mo_4Al_{43}$. These three alloys were irradiated with 2.6 MeV protons at 200°C to doses of 0.1, 1.0, and 3.0 dpa. Initial TEM benchmarking has been completed and included identifying the structures of each phase and bright-field imaging of each phase to show any defects that might be present during casting. Analysis of the proton-irradiated samples has been initiated and the alloys show little to no changes in microstructure in most phases under the specified irradiation conditions.

1. Introduction

To address the public concern of nuclear proliferation, the Reduced Enrichment for Research and Test Reactors (RERTR) fuel development team was tasked with developing new low-enriched uranium (LEU) fuels that can replace currently used highly-enriched uranium (HEU) fuels in many research and test reactors throughout the world. The current LEU designed fuel is a dispersion fuel, which is composed of a U,Mo fuel kernel embedded in an Al-matrix. Neutron irradiation tests of these fuels have shown unacceptable fuel performance at high burnup. An important part of developing this fuel is understanding its in-reactor performance. For the dispersion fuel, the radiation stability of the interaction layer that forms between the fuel kernel and the Al-matrix plays the major role in fuel behavior and performance. It is believed that by proton irradiating these fuels at low doses, insights on the microstructure stability of the interaction layer can be studied. Proton irradiations provide a low cost, fast, and low activation method to study the microstructure changes with irradiation damage.

Irradiations and diffusion couple tests of RERTR dispersion fuels have shown that many phases form in the interaction layer of a (U,Mo)/Al dispersion fuel. Mazaudier et al. [1] has shown in a U-xMo (x=5, 7, and 10 wt%) system, a complex three-layered interaction layer is formed in heat treated diffusion couples. Each of these layers formed specific phases ranging from UAl_3, UAl_4, UMo_2Al_{20}, and $U_6Mo_4Al_{43}$. To help understand the microstructural stability of the various phases, three depleted uranium (DU) alloys were cast to establish these phases for the proton irradiations. The compositions of the alloys in wt% were 67U-5Si-28Al (alloy-A), 48U-5Mo-47Al (alloy-B), and 69U-4Mo-20Al-7Si (alloy-D). The primary phase seen in alloy-A is $U(Al,Si)_3$. This phase has been seen in the uranium-silicide dispersion fuel program in the interaction layer. This phase has a stable irradiated microstructure and will be used as a benchmark of comparison for the other phases present in the alloys. Alloy-B contains the UAl_4, UMo_2Al_{20}, and $U_6Mo_4Al_{43}$ phases seen in typical UMo-Al dispersion fuel. Because of the early issues in the RERTR with unstable interaction layer growth, Si additions to the Al-matrix have been explored to help reduce this layer growth. Additions of 2 wt% Si in Al cladding have been shown to greatly reduce the interaction layer thickness and form the $(U,Mo)(Al,Si)_3$ phase in this region [2]. Alloy-D was cast to simulate this phase.

The primary objective of the proton irradiations is to study the microstructural response of these phases under proton irradiations. This includes seeing if UAl_4, UMo_2Al_{20}, and $U_6Mo_4Al_{43}$ perform poorly during irradiation, if $U(Al,Si)_3$ performs well during irradiation, and understanding how $(U,Mo)(Al,Si)_3$ behaves with irradiation in comparison to $U(Al,Si)_3$. It is hoped that $(U,Mo)(Al,Si)_3$ will respond similarly to the $U(Al,Si)_3$ phase as seen in the silicide fuels [3]. Microstructural analysis, using TEM, will consist of characterizing the radiation stability, amorphization, cavity formation and distribution of defects as a function of radiation dose.

2. Experiment

The three DU alloys for proton irradiations were cast using arc melting. High purity Al, Mo, and Si at 99.999% were used for alloy fabrication. The cast ingots were wrapped in a Ta foil, sealed in a stainless steel tube, and homogenized at 500ºC for 200 hours. Each ingot weighed approximately 15 grams. Table 1 lists the material information for each alloy.

Table 1: DU Alloys Cast for Proton Irradiation Studies

Alloy Designation	A	B	D
Composition (wt%)	67U-5Si-28Al	48U-5Mo-47Al	69U-4Mo-20Al-7Si
Composition (at%)	$U_{19}Si_{12}Al_{69}$	$U_{10}Mo_3Al_{87}$	$U_{22}Mo_3Al_{56}Si_{19}$
Phases Present	$U(Al,Si)_3$	UMo_2Al_{20}, UAl_4, $U_6Mo_4Al_{43}$	$(U,Mo)(Al,Si)_3$, UMo_2Al_{20}
Found in Fuel Type	(U,Si)/Al Fuel	(U,Mo)/Al Fuel	(U,Mo)/(Al,Si) Fuel
Anticipated Performance	Good	Not Good	Good
Microstructural Stability	Stable	Cavity and Swelling	Stable (?)

To ensure that the castings contained the appropriate phases, scanning electron microscopy (SEM) analysis was performed to identify the phases present. A ZEISS Model 960A SEM with an Oxford wavelength dispersive spectrometer (WDS) and an

energy dispersive spectrometer (EDS) that employed ISIS LINK software was used for analysis. Secondary electron images were obtained to show the microstructure of the material and can be seen below in Figure 1. In addition, WDS and EDS were used to provide X-ray maps and point compositions along the microstructure. SEM analysis showed that the phases of interest were present in their respective cast alloy.
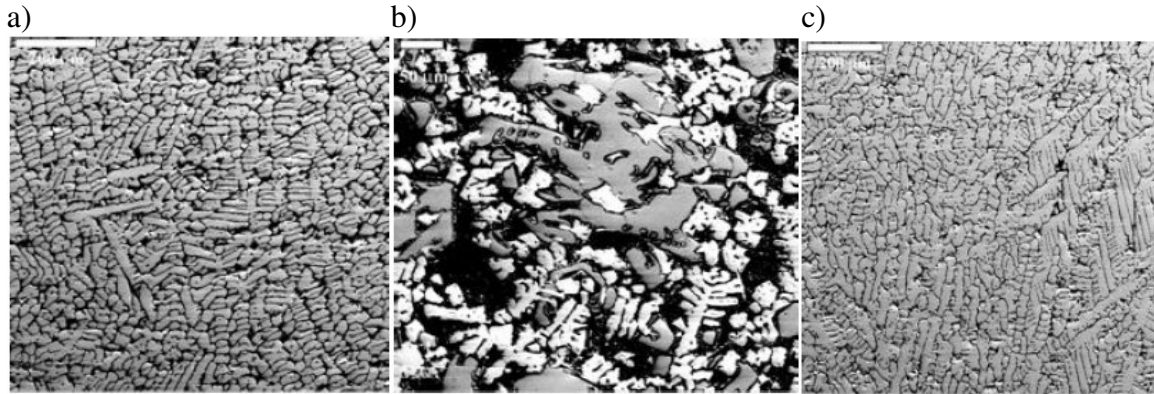
a)   b)   c)

Figure 1: a) Microstructure of Alloy A. b) Microstructure of Alloy B. c) Microstructure of Alloy D. (The size of the scale bar is 200μm, 50μm, 200μm for image (a), (b) and (c), respectively)

For the proton irradiations, the cast alloys were cut into 300-400 μm thick slices using a low speed saw. 3.0 mm-diameter TEM disks were core drilled from the thin slices. The discs were mechanically wet polished to a finish of 1200 grit on one side and to 600 grit on the other side. The 1200 grit polished side was the side being irradiated by the protons. The 600 grit side was not polished to 1200 grit to act as a mechanism to identify which side was irradiated by the protons. Proton irradiations were conducted at the University of Wisconsin-Madison using a 1.7 MeV tandem accelerator made by NEC. Averages of 12-15 discs were mounted onto the irradiation stage. An indium foil was placed between the sample well of the stage and the samples to provide a liquid interface to improve thermal conduction during irradiation. Irradiations were done using a 2.6 MeV proton beam rastered over a 10x16 mm^2 area to provide a uniform dose to each sample. Irradiation temperature was monitored by the use of three thermocouples mounted to the stage and by the use of an IR camera capable of monitoring the temperature on each sample. The temperature was controlled at 200±20ºC. The displacement per atom (dpa) rate was estimated to be approximately 7.0×10^{-6} dpa/s using SRIM 2006 calculations using the default displacement energy of 25 eV for a metal [4], which corresponds to roughly 1 dpa per 25 hours. The protons have a range of roughly 40-50 μm into the alloys. The alloys were irradiated to doses of 0.1, 1.0, and 3.0 dpa.

To create a TEM transparent sample, the proton irradiated disc samples were back thinned on the unirradiated side to a final thickness of roughly 100-150 μm. Samples were jet polished using a single jet polisher with a solution of 5% perchloric acid in methanol at -45ºC using an applied voltage around 90V. The samples were jet polished on the proton irradiated side for 5 seconds to remove any surface contamination and then flipped over to the unirradiated side and polished to perforation. This created a TEM area that has a relatively constant damage profile and is the location where the damage rate

was used for the dpa calculations. In most samples, additional thinning is required to create a large TEM area for analysis. This was accomplished by use of a Gatan PIPS ion milling system. Typical ion polishing times were around 30 min to 2 hrs using a 4 keV Ar beam.

3. Results

Prior to analyzing the proton irradiated alloys, benchmarking of the unirradiated alloys was conducted. Analysis was conducted to verify the SEM results and to serve as a reference of comparison for the irradiated alloys. In each alloy, EDS was used to verify the compositions of the phases present. Diffraction patterns were obtained to verify the phase's structure and bright field images were obtained to show any defects present in phases and overall structure of the phases. In addition to these techniques, lattice fringe imaging was conducted on phases with large lattice parameters. EDS on the samples presents an issue in the alloys. When conducting EDS measurements it was found that measurements were needed to be conducted at the thinnest location on the grains. When EDS was conducted in thicker areas in the grains, U composition would increase and Al concentration would decrease. This is due to the uranium shielding and absorption of gamma rays. EDS measurements verified the results seen in the SEM analysis.

Two phases exist in Alloy A: $U(Al,Si)_3$ and Al. $U(Al,Si)_3$ composes the majority of the alloy with the Al appearing in small pockets throughout the material as seen in SEM analysis. This is the primary phase seen in uranium-silicide fuel. The $U(Al,Si)_3$ phase shows a superordered lattice structure, $L1_2$ ordered simple cubic, as shown in Figure 2a. Bright field (BF) images show a defect clean structure as seen in Figure 2b.
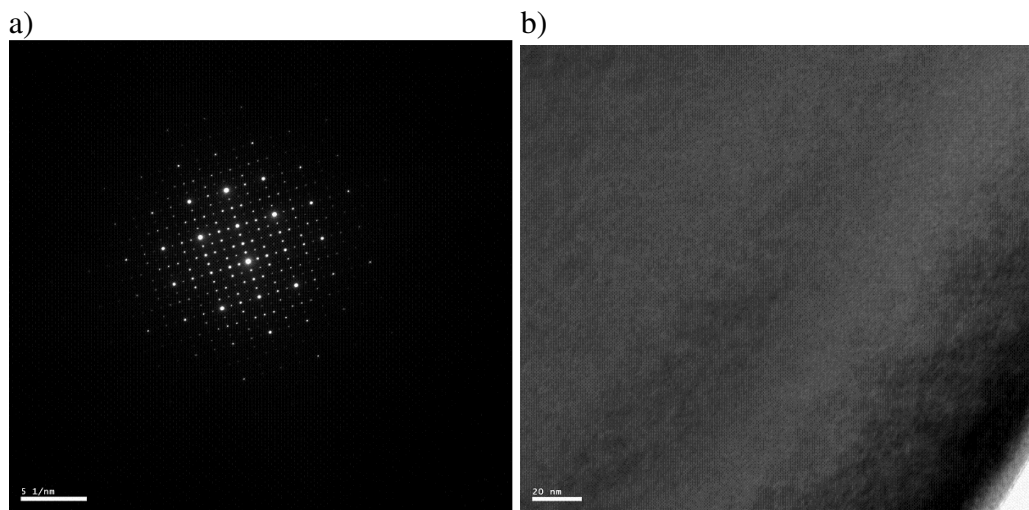
a)   b)

Figure 2: a) Superordered Diffraction Pattern (z=100) of $U(Al,Si)_3$. b) Bright field image of the microstructure of $U(Si,Al)_3$ at 100kX showing no defects

Alloy B is composed of four phases: UMo_2Al_{20}, UAl_4, $U_6Mo_4Al_{43}$, and Al. These phases represent the phases expected to form in the (U,Mo)/Al dispersion fuel interaction layer. TEM sample preparation required ion milling times of greater than 6 hours to create a useable TEM sample. $U_6Mo_4Al_{43}$, hexagonal structure, showed a relatively clean structure and lattice fringe images were obtained and can be seen in Figure 3a. UMo_2Al_{20}

shows an interesting microstructure, forming nano-sized grains throughout the structure. Imaging these grains show high density of stacking faults throughout the material. This can be seen in Figure 3b.
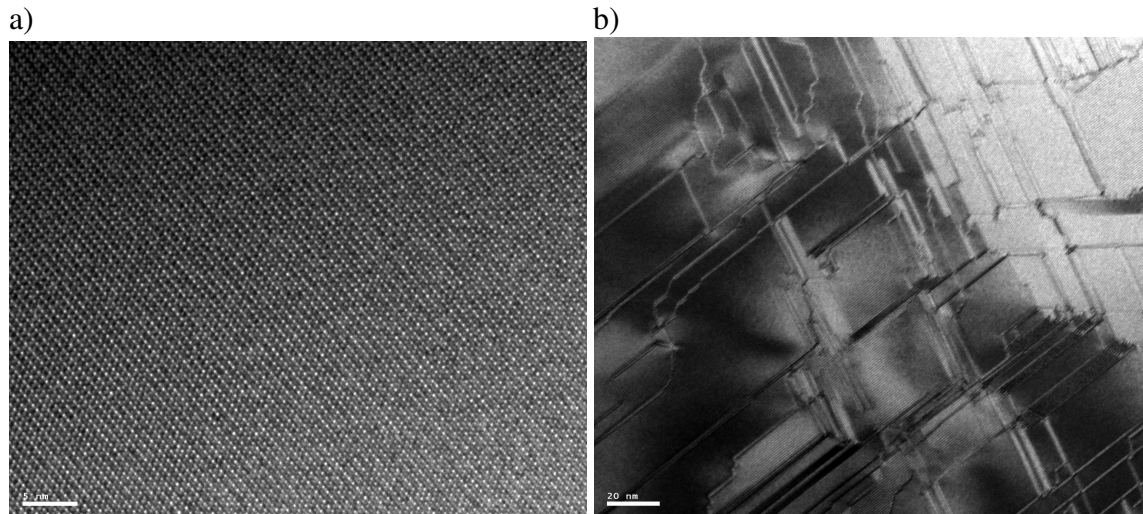
a)   b)

Figure 3: a) Lattice fringe image of $U_6Mo_4Al_{43}$ at 400kX. b) BF image showing stacking faults in UMo_2Al_{20} at 100kX.

UAl_4 contains unknown precipitates throughout all of the UAl_4 grains, body-centered orthorhombic structure. These defects can be seen in Figure 4. These defects are too small to use EDS with and show no extra spots in diffraction patterns. They are sensitive to tilt but do not totally disappear once off a 2-beam condition like dislocation loops. The precipitates from the proton irradiated alloys are larger in size and EDS measurements show that the precipitates are U-Mo-Al in composition and extra diffraction spots in the diffraction patterns can be seen.
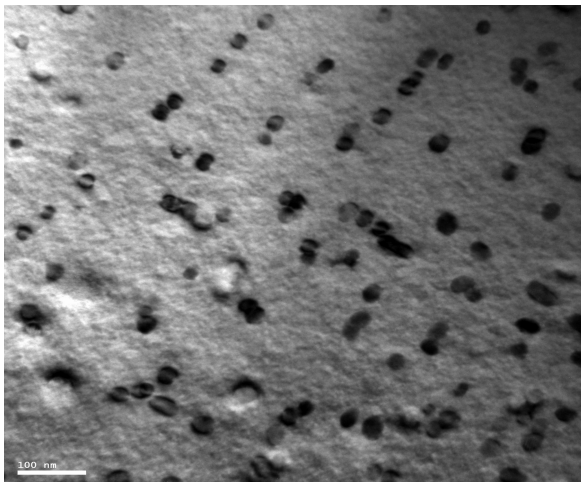

Figure 4: BF image showing the nano-sized precipitates present throughout unirradiated UAl_4 grains.

Alloy D has three phases present: $(U,Mo)(Al,Si)_3$, UMo_2Al_{20}, and Al. The $(U,Mo)(Al,Si)_3$ phase, $L1_2$ ordered structure, shows a clean unirradiated microstructure as seen in Figure 5a. The UMo_2Al_{20} phase shows stacking faults at a much lower density than that seen in the UMo_2Al_{20} phase in Alloy B and its lattice fringe image can be seen in Figure 5b.
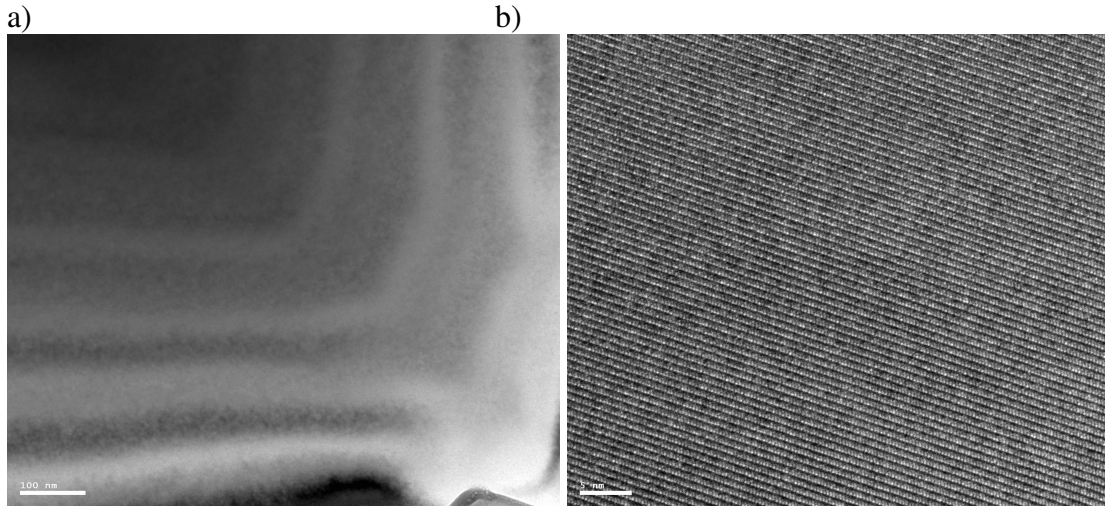
a)   b)

Figure 5: a) BF image of $(U,Mo)(Al,Si)_3$ showing a clean microstructure at 25kX. b) Lattice fringe image of UMo_2Al_{20} at 400kX.

3.1   Proton Irradiated Alloys:

TEM analysis on the proton irradiated alloys has been initiated. Initial study has shown little to no defects are present in alloys A and D. The only proof of irradiation can be seen in the form of large rectangular faceted voids present in the Al phases. The large voids and low density are likely due to the irradiation temperatures. It is at the high end of the void formation regime (T/T_m=0.5), leading to large voids and low densities. An image of the voids can be seen in Figure 6.
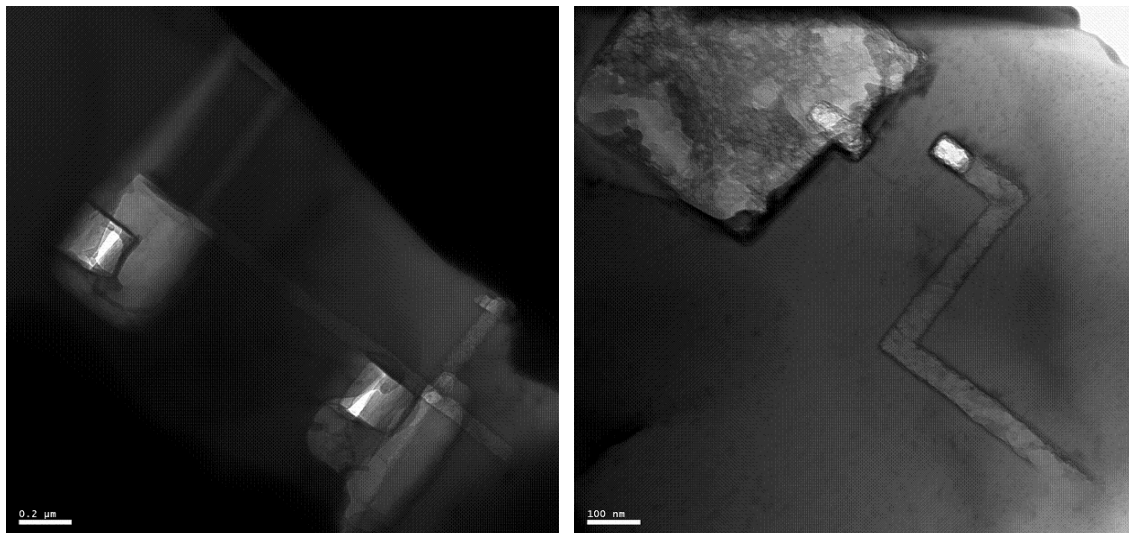

Figure 6: Voids present in the microstructure of Al in alloy D at 1.0 dpa

In alloy B, UAl_4 shows potential radiation damage. The precipitates seen in the unirradiated fuel have decreased in density and have formed larger precipitates (coarsening) with increasing dose. This evolution can be seen in Figure 7. It is believed at the present time that this is radiation induced. With the increase in size of these precipitates, EDS measurements were used to show that Mo was present in these precipitates, indicating the formation of an unknown precipitate phase through UAl_4. Additionally, diffraction patterns of the precipitates show small satellite spots around the higher order UAl_4 spots. At the current time it is unknown what these precipitates are, but it is believed that these precipitates could be UMo_2Al_{20} from the EDS measurements.
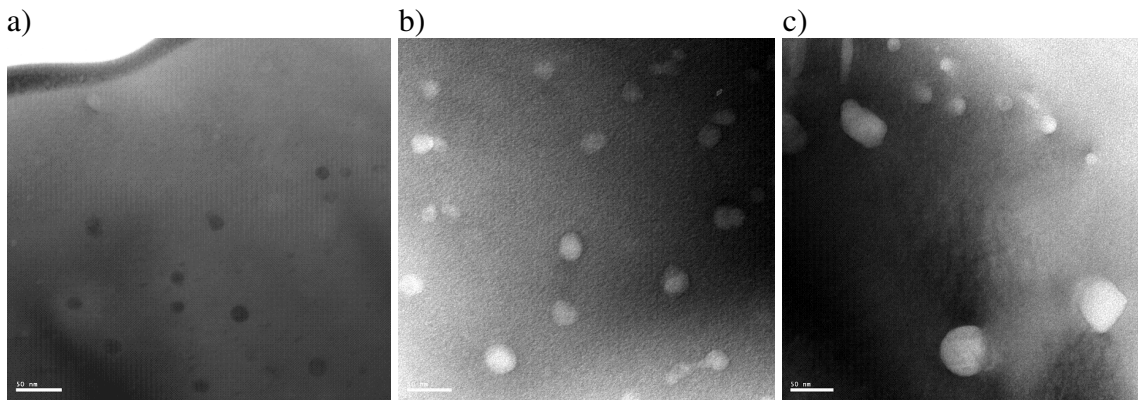
a)   b)   c)

Figure 7: Evolution of U-Mo-Si Precipitates in UAl_4 with increasing dose: a) unirradiated b) 1.0 dpa c) 3.0 dpa (Scale bar is 50 nm)

4. Discussion

Initial benchmarking of the phases in the proton-irradiation alloys show most have relatively clean microstructures. UMo_2Al_{20} is present in Alloy B and D with both alloys showing different pre-irradiated microstructures. In alloy B, many stacking faults are present in the material with a nano-sized grain structure. In alloy D, the UMo_2Al_{20} grains are on the μm-sized level and show very few stacking faults. This is likely due to the difference in the development of the UMo_2Al_{20} phase between alloy B and alloy D. Another interesting effect in the alloys is the transition of $U(Al,Si)_3$ from a superlattice ordered $L1_2$ structure to standard $L1_2$ ordered structure with the addition of Mo to the structure as seen in $(U,Mo)(Al,Si)_3$. The UAl_4 phase in Alloy B shows a large density of U-Mo-Al type precipitates. These precipitates are believed to be incoherent due to the absence of extra diffraction spots in UAl_4 diffraction patterns.

Analysis of the proton irradiated fuel has begun. Analysis of Alloy A and D show very little irradiation defects are present besides the formation of large, low-density voids in aluminum. It is believed that lack of defects visible on the TEM scale is a result of the relatively low irradiation temperature. In UAl_4, the nano-sized precipitates found in the unirradiated alloys have formed larger Mo rich U-Mo-Al type precipitates during irradiation. It is believed that this is due to irradiation since the temperature is too low for thermal process. Additional work will be conducted on these alloys to verify these results. With the lack of radiation damage in these phases, it is possible that the irradiation conditions were not favorable for producing meaningful defect

microstructures or that the alloys are stable to neutron/proton damage. It suggests that the microstructural behavior of these phases in the reactor may be dominated by the fission product damage.

5. Conclusion

TEM analysis on three proton irradiated simulated interaction layers has started. Benchmark TEM analysis of the three alloys shows the expected phases to be present and chemical information, structural information, and reference images were obtained for comparison with the proton-irradiated alloys. TEM analysis on the proton-irradiated fuel is being conducted and initial work shows little to no radiation damage in most phases present in the alloys. UAl_4 shows growth of precipitates with increasing dose.

6. Future Work

Future work will include additional proton irradiations with different irradiation parameters to hopefully see radiation damage in these alloys. Heavy ion irradiations will be conducted at Intermediate Voltage Electron Microscopy (IVEM) at the Argonne National Laboratory to simulate fission product damage. Kr^+ ions will be used at 200°C to doses of 1 dpa and 10dpa.

7. References

[1] F. Mazaudier, C. Proye, F. Hodaj, "Further Insight into Mechanism of Solid-State Interactions in UMo/Al System", J. of Nucl. Mater., 377 (2008) 476-485.
[2] G. Hofman, Y. Kim, H. Ryu, and M. Finlay, "Improved Irradiation Behavior of Uranium-Molybdenum/Aluminum Dispersion Fuel", Proceedings of the International Meeting on RRFM, Lyon, France, Mar. 11-15, 2007.
[3] Y.S. Kim, G. L. Hofman, H. J. Ryu, J. Rest, "Thermodynamic and Metallugical Considerations to Stabilizing the Interaction layers of U-Mo/Al Dispersion Fuel", Proceedings of the International Meeting on RERTR, Boston, USA, Nov. 6-10, 2005.
[4] J. Zeigler, TRIM 2008 Manual, http://www.srim.org/SRIM/SRIM%2008.pdf